

**Discovering the Potential Mechanisms of *Canna indica* Leaves Ethanolic Extract against *Plasmodium falciparum* Malaria: Network Pharmacology and Molecular Docking Approach**Kana Mardhiyyah^{1*}, Christopher K. Johan², Eurica A. N. Ravsanjani²¹Department of Biochemistry & Biomolecular, Faculty of Medicine, University of Brawijaya, Malang, Indonesia.²Department of Pharmacy, Faculty of Medicine, University of Brawijaya, Malang, Indonesia.

ARTICLE INFO

Article history:

Received 31 December 2024

Revised 02 January 2025

Accepted 15 February 2025

Published online 01 March 2025

ABSTRACT

Malaria is a life-threatening disease caused by *Plasmodium* parasites and transmitted by *Anopheles* female mosquito. *Plasmodium falciparum*, one of the most common and deadliest species, accounting for more than 99% cases of malaria-associated deaths globally. Several therapy strategies which often involves quinolones and artemisinin derivatives have been used. However, new challenge arises due to the exceptional adaptability of *P.falciparum* towards antimalarial drugs that leads to the failure of malaria therapy. This study investigates the antimalarial potential of *Canna indica* leaves ethanolic extract against *Plasmodium falciparum* using network pharmacology and molecular docking approaches. A total of 57 phytoconstituents were identified in the ethanolic extract of *C. indica* and were screened for pharmacokinetic properties, resulting in 46 eligible compounds for further analysis. Protein-protein interaction (PPI) network and pathway analyses identified key targets, including acetylcholinesterase (AChE), sex hormone-binding globulin (SHBG), prostaglandin-endoperoxidase synthase (PTGS2), coagulation factor X (F10), and butyrylcholinesterase (BuChE). Molecular docking results demonstrated significant binding affinities of *C. indica* compounds with the target proteins, including AChE, SHBG, PTGS2, F10, and SHBG along with the lowest binding affinity values of -9.2 kcal/mol, -8.6 kcal/mol, -7.8 kcal/mol, -7.7 kcal/mol, and -10.6 kcal/mol respectively. This finding suggests that *C. indica* possesses bioactive compounds that could serve as candidates for novel antimalarial therapeutics.

Copyright: © 2025 Mardhiyyah *et al.* This is an open-access article distributed under the terms of the [Creative Commons Attribution License](https://creativecommons.org/licenses/by/4.0/), which permits unrestricted use, distribution, and reproduction in any medium, provided the original author and source are credited.

Keyword: *Canna indica*, Antimalarial, *Plasmodium falciparum*, Network pharmacology, Molecular docking.

Introduction

Malaria is a life-threatening disease and transmitted by *Anopheles* female mosquito.¹ In 2022, nearly half of the world's population is at risk of malaria, including sub-Saharan Africa which carries a high share of malaria burden globally followed by South-East Asia, Eastern Mediterranean, Western Pacific, and Americas. A total of 247 million malaria cases were recorded in the World Malaria Report 2022, showing a significant increase compared with 229 million global cases reported in 2019, with 94% of its cases was recorded in Africa.^{2,3} Approximately 120 *Plasmodium* species, a single-celled parasite as the causative agent of malaria, are identified, but only five species may cause malaria in humans: *Plasmodium falciparum*, *Plasmodium vivax*, *Plasmodium ovale*, *Plasmodium malariae*, and *Plasmodium knowlesi*. Among other species, *P. falciparum* is considered as the most common and deadliest species, accounting for more than 99% cases of malaria-associated deaths globally.⁴ To overcome this, several therapy strategies which often involves quinolones and artemisinin derivatives have been used.

*Corresponding author. Email: kanamardhiyyah@ub.ac.id
Tel: +6285649287041

Citation: Mardhiyyah K, Johan CK, Ravsanjani EAN. Discovering the Potential Mechanisms of *Canna Indica* Leaves Ethanolic Extract against *Plasmodium Falciparum* Malaria: Network Pharmacology and Molecular Docking Approach. Trop J Nat Prod Res. 2025; 9(2): 702 – 710 <https://doi.org/10.26538/tjnpr/v9i2.37>

Official Journal of Natural Product Research Group, Faculty of Pharmacy, University of Benin, Benin City, Nigeria

However, new challenge arises due to the swift adaptability of *P.falciparum* towards antimalarial drugs that leads to the failure of malaria therapy. Therefore, novel therapeutic intervention is necessary to tackle antimalaria drug resistance.⁵ Over the past half-century, natural products have proven to provide powerful therapeutics against infectious disease. For example, artemisinin as one of the most effective treatments against malaria is a natural constituent of *Artemisia annua*. In addition, utilizing natural compounds as novel treatment offers promising benefits including minimal side effects and cost-effective.⁶ *Canna indica* of the *Cannaceae* family is known for its extensive use as traditional medicine due to the antioxidant, antibacterial, anti-inflammatory, antimicrobial, immunomodulatory, and analgesic activities, hence becoming one of the novel candidates for antimalarial drugs.⁷ However, studies exploring the mechanism of *C. indica* especially in molecular level remains under-researched. Therefore, *in silico* approach utilizing bioinformatic systems, network pharmacology and molecular docking, are needed to predict and understand the biological activities of *C. indica*.

Network pharmacology is a novel approach in computational biology studies aiming to reveal biomolecular interactions between bioactives and its target proteins. Initially utilized in discovering complex pharmacological mechanisms of multicomponent-possessing Traditional Chinese medicine (TCM), network pharmacology has been widely utilized in the early stage of drug development.⁸ Previous study reported the pharmacological mechanisms of *Saussurea lappa* in alleviating viral respiratory diseases by inhibiting several key inflammatory markers, including nuclear factor-kappa B (NF-κB).⁹ Network pharmacology was also utilized to uncover the mechanism of bioactives from *Chypomandra betacea* in treating type 2 diabetes mellitus through several pathways, including AGE-RAGE signaling pathway and insulin resistance-related processes.¹⁰ In the other hand, molecular docking is a technique utilized to discover potential drug

candidate by predicting the binding mechanism, affinity, and interactions of a ligand to a target receptor of interest.¹¹ Molecular docking method was able to disclose the molecular interaction of quercetin with IgE in individuals, as performed in another study.¹² Hence, these methods are suitable to provide analytical results and insights on the activity of *C.indica*'s metabolite as a novel antimalarial agent. To date, no research has been conducted to study the activity of *C. indica* as antimalarial agent by combining the application of network pharmacology and molecular docking. Therefore, the main purpose of this study is to discover the potential antimalarial activities of several metabolites identified in *C. indica* in molecular level and providing novel nature-based therapeutic options to combat malaria.

Materials and Methods

Materials

Phytoconstituents of the ethanolic extract of *Canna indica* leaves were obtained from LC/MS analysis conducted by Nugraha *et al.*¹³ This *in silico* study was performed using AMD Ryzen 7 processor with 8GB RAM. Software utilized were including Cytoscape 3.10.0 (manufactured 2023 by the Cytoscape Team), PyMOL 2.5. (released 2021 by the Schrödinger, Inc.), OpenBabel 3.0.1. (released 2019 by the Open Babel Team), PyRx 0.8 (developed 2010), and BIOVIA Discovery Studio v24.1.0.23298 (manufactured 2024 by Dassault Systeme BIOVIA). Several online websites and databases, namely PubChem (<https://pubchem.ncbi.nlm.nih.gov/>), SwissADME (<http://www.swissadme.ch/>), Swiss Target Prediction (<http://www.swisstargetprediction.ch/>), GeneCards (<https://www.genecards.org/>), SRplot (https://www.bioinformatics.com.cn/login_en), STRING (<https://string-db.org/>), Metascape (<https://metascape.org>), RCSB Protein Data Bank (<https://www.rcsb.org/>), MolProbity (<http://molprobity.biochem.duke.edu/>), and Zhang Lab's DockRMSD (<https://zhanggroup.org/DockRMSD/>) were also used in this study.

Data collection and pharmacokinetic screening

Simplified Molecular-Input Line-Entry System (SMILES) of each *C. indica* phytoconstituents were retrieved from PubChem. Pharmacokinetic attributes of the compounds, including molecular weight (MW), hydrogen bond donor (HBD), hydrogen bond acceptor (HBA), clogP, Topological Polar Surface Area (TPSA), and bioavailability were obtained by inputting their respective SMILES in SwissADME. Screening was conducted according to Lipinski's rule of five, where compounds with available SMILES, ≤ 1 Lipinski's rule violation, $< 140\text{\AA}$ TPSA, and $> 10\%$ bioavailability score are considered eligible for further analysis.¹⁴⁻¹⁶

Core protein targets retrieval and protein-protein interaction (PPI) network analysis

Phytoconstituents target prediction was predicted using Swiss Target Prediction (STP), while GeneCards was used to obtain malaria-related targets. Common targets of these two domains were intersected using Venn diagram model constructed through SRplot. The obtained core targets were constructed as PPI network performed through STRING and further analyzed using Cytoscape 3.10.0 software.^{17,18}

Gene Ontology (GO) & Kyoto Encyclopedia of Genes and Genomes (KEGG) enrichment analysis

Further confirmation of the previous findings was conducted using GO-KEGG enrichment analysis. Core targets obtained were inputted through Metascape by setting *Homo sapiens* prior to the analysis.^{17,19,20}

Herbs-Compounds-Targets-Pathways-Diseases (H-C-T-P-D) network analysis

H-C-T-P-D network was constructed to predict the interactions between *C. indica*, phytoconstituents, core target proteins, pathways, and diseases using Cytoscape 3.10.0. Degree analysis was conducted using the software. Compounds with the highest three degree and targets with the top six degree were identified for further analysis.^{17,21}

Structure preparation and geometric validation

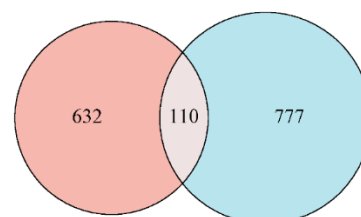
Three-dimensional structures of the obtained compounds were retrieved from PubChem in SDF format, which was converted using OpenBabel 3.0.1. to obtain the PDB format. Furthermore, crystal structures of each target proteins described in previous research were retrieved from RCSB Protein Data Bank.¹³ Proteins were sterilized from its water and native ligand, and validated geometrically using Ramachandran favored score calculated in MolProbity, where $>90\%$ score is considered ideal for further assessment.²²

Molecular docking and visualization

Molecular docking simulation was performed using PyRx 0.8. Binding affinity of each ligand-protein interaction was used as a bond stability indicator. Furthermore, docked native ligand was calculated for its pose distance using Zhang Lab's DockRMSD, where root mean square deviation (RMSD) score $\leq 5\text{\AA}$ indicate small deviation between the ligand's natural pose and binding conformation.²³ The obtained compounds in their respective binding pose were docked to the macromolecule structure using PyMOL 0.8. Amino acid interactions obtained were visualized and illustrated using BIOVIA Discovery Studio v24.1.0.23298. Higher number of matching amino acid interactions compared to each target and their respective natural ligands interaction indicate similar molecular interaction was observed.²⁴

Results and Discussion

57 compounds obtained from LC/MS analysis in a previous study were screened, resulting in a total of 46 eligible compounds.¹³ Five compounds were eliminated due to unaccessible SMILES, while the remaining six compounds were ineligible due to > 1 violations in Lipinski's rule of five or incomplete pharmacokinetic data predicted. A total of 742 compound-related targets and 887 disease-related targets were obtained from STP and GeneCards, respectively. Furthermore, Venn diagram model of compound- and disease-related targets revealed 110 common targets between the two domains (**Figure 1**). PPI network illustrating interaction between common targets were constructed using STRING (**Figure 2**). Top 20 proteins in the network were identified using CytoHubba plug-in, where CASP3, TNF, MMP9, ICAM1, TLR4, VCAM1, IL6, SELE, and PTGS2 possess 19 degrees each (**Figure 2(b)**).



Compound-related Targets Malaria-related Targets

Figure 1: Venn Diagram of the Common Targets

GO-KEGG enrichment analysis revealed 351 biological processes (BP), 47 cellular components (CC), and 11 molecular functions (MF) as shown in **Figure 3**. Furthermore, 42 related pathways were identified and 10 pathways with the lowest p-value were illustrated in **Figure 4**. Three top results from KEGG analysis were AGE-RAGE, NF- κ B, and IL-17 signaling pathways. Aligned results were reported in previous research, in which high intake of AGE-rich cooked foods triggers chronic RAGE activities and maintains long-term inflammation in several infectious disease including malaria.²⁵ NF- κ B signaling pathway was also reported as a core regulator in immune response elicited against *Plasmodium* infection. Recent findings demonstrated that p65 translocation and I κ B degradation in the nucleus of neurons, leukocytes, and glial cells was significantly elevated in severe and cerebral *P. falciparum* malaria patients, suggesting NF- κ B role in regulating inflammatory response during malaria progression.²⁶

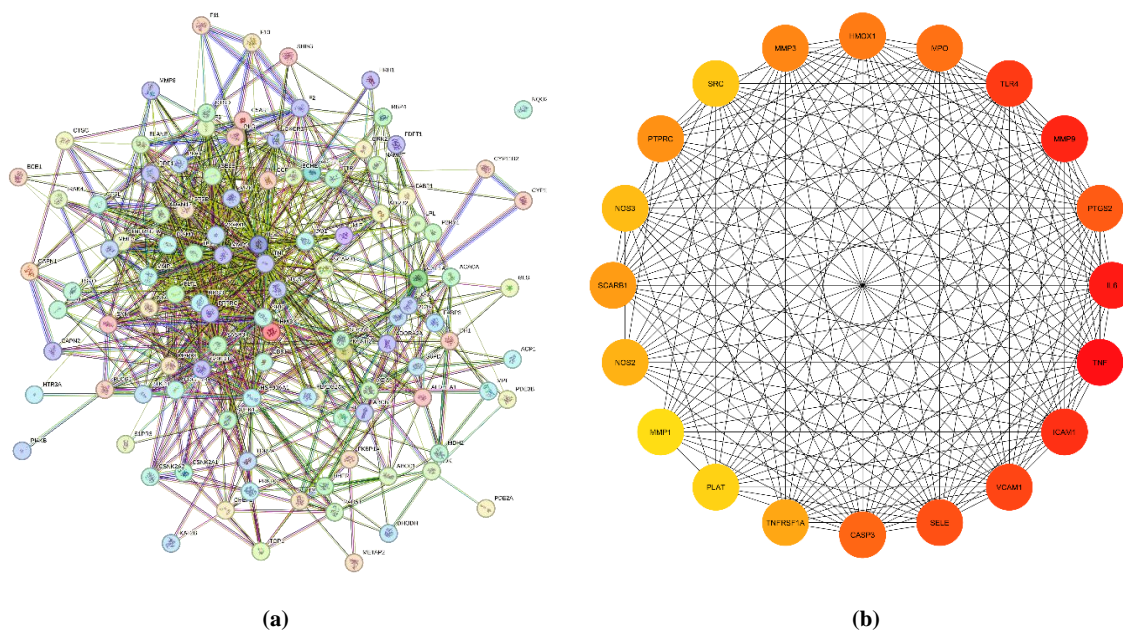


Figure 2: (a) PPI Network of 110 Core Targets; (b) PPI Cluster Consisting Top 20 Proteins

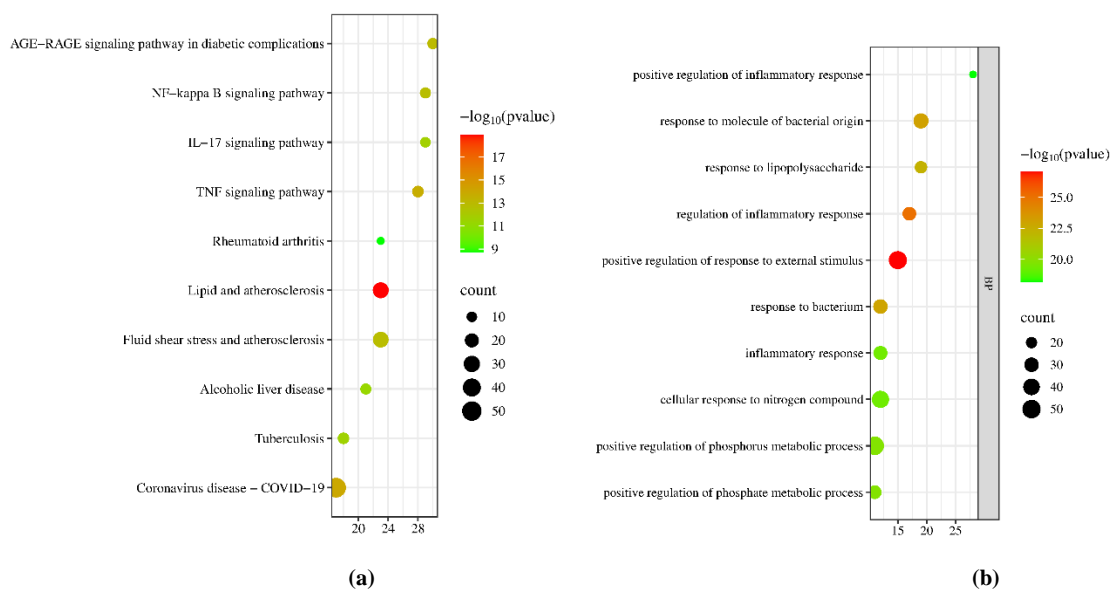


Figure 3: (a) KEGG; (b) GO Bubble Plot Analysis

IL-17 was also found to surge in acute *P. falciparum* malaria infection, IL-17 was suspected to regulate adaptive mechanisms against changing blood viscosity.^{27,28} Increase in blood viscosity due to decreased erythrocyte deformability is another clinical manifestation in malaria, corroborating GO result described in Figure 3b.²⁹

Herbs-compound-target-pathway-disease (H-C-T-P-D) network was constructed as seen in Figure 5. Green hexagon symbolizes *Canna indica*, orange ellipses represent the phytoconstituents, blue circles represent the core targets, red rectangle symbolizes malaria, while the green rectangles represent related pathways. Subsequently, targets with six highest degrees, namely ACHE (26), SHBG (23), PTGS2 (22), CTSL (19), F10 (19), and BCHE (19), as well as compounds with the three highest degrees (2-(phenylmethylene)-octanal (25), 3',8,8'-trimethoxy-3-piperidyl-2,2'-binaphthalene-1,1',4,4'-tetrone (23), nootkaton-11,12-epoxide (22), and 2-(4a,8-Dimethyl-6-oxo-1,2,3,4,4a,5,6,8a-octahydro-naphthalen-2-yl)-propionaldehyde (22)

possessed significant role in the network and were selected for further molecular docking analysis.

Molecular docking results are presented in Table 1. Docking grid box scale was set as described in Table 2, while binding affinity and amino acid residues are shown in Table 3. Docked bioactives visualization are illustrated in Figure 6-10. As seen in Table 3, 2-(4a,8-Dimethyl-6-oxo-1,2,3,4,4a,5,6,8a-octahydro-naphthalen-2-yl)-propionaldehyde produces the most stable bond against AChE protein, demonstrated by the lowest binding affinity compared to the other phytoconstituents. 3',8,8'-Trimethoxy-3-piperidyl-2,2'-binaphthalene-1,1',4,4'-tetrone generated the highest number of matching amino acid interactions with AChE despite having the highest binding affinity value (Table 4 & Figure 6).

Table 1. Protein Identity

Protein Identity	PDB ID	Ramachandran	DockRMSD
Human acetylcholinesterase (ACHE)	4EY7	97.33%	0.378
Sex Hormone Binding Globulin (SHBG)	1KDM	91.43%	0.448
Prostaglandin Synthase 2 (PTGS2)	5F19	96.89%	0.803
Coagulation Factor X (F10)	5VOF	97.36%	0.547
Butyrylcholinesterase (BCHE)	4BDS	96.15%	4.791

Table 2. Grid Box Scale of Molecular Docking

Target	Native	Center Grid Box			Grid Size		
		X	Y	Z	X	Y	Z
ACHE	E20	-14.724	-44.9484	27.3877	17.1220	8.9163	13.4014
SHBG	DHT	-6.2613	38.9716	31.8363	11.2838	11.0890	8.0178
PTGS2	COH	27.8275	30.2581	63.3145	15.4417	12.2940	13.9652
F10	RIV	-4.5402	-20.7495	-4.3482	24.5990	18.7592	10.207
BCHE	THA	134.8567	118.4827	40.9791	15.6271	14.5469	12.302

Table 3. Binding Affinity Results

Compound	Binding Affinity (kcal/mol)				
	ACHE	SHBG	PTGS2	F10	BCHE
2-(4a,8-Dimethyl-6-oxo-1,2,3,4,4a,5,6,8a-octahydro-naphthalen-2-yl)-propionaldehyde	-9.2	-8.6	-6.2	-6.7	-7.8
3',8,8'-Trimethoxy-3-piperidyl-2,2'-binaphthalene-1,1',4,4'-tetrone	-6.7	8.7	-7.8	-7.7	-10.6
Nootkaton-11,12-epoxide	-8.9	-8.4	-7.3	-6.5	-8.0
Octanal, 2-(phenylmethylene)-	-8.1	-7.5	-7.4	-6.6	-6.9
Native	-12.2	-12.2	-12.5	-9.3	-8.2

To the best of our knowledge, current preclinical and clinical studies are lacking evidence on the definite role of AChE in malaria pathophysiology. However, certain study reported that AChE as a novel target for donepezil-derived insecticide. This study revealed excellent selectivity of several derivatives obtained from donepezil structural modification in suppressing human and *Anopheles* AChE, demonstrated by different residues involved (His447, Trp279, and Trp286 in human vs Trp245, Gly278, Tyr483 in *Anopheles gambiae*).³⁰ Similar study also reported interesting findings, where artemisinin, the first-line pharmacological management of malaria, demonstrated excellent inhibitory activity against AChE with an IC₅₀ value of 29.34 µg/mL, indicating its role in limiting several AChE-related neurological disorders.³¹ Therefore, these findings may reveal potential AChE modulation pathway as an antimalarial mechanism of *Canna indica* bioactives.

2-(4a,8-Dimethyl-6-oxo-1,2,3,4,4a,5,6,8a-octahydro-naphthalen-2-yl)-propionaldehyde was also found to generate the lowest binding affinity (-8.2 kcal/mol) and five matching residues against SHBG (Figure 7). Sex hormone-binding globulin (SHBG) activities in malaria were found

to compose the native ligand of TAM receptors and AXL activities. Its key member, AXL, was discovered to contribute in immunosuppressive cells differentiation, hemolysis, and hypoxia in malaria cases, therefore the modulation of SHBG activity may intervene the stability of AXL and exert antimalarial activity.³² While limited preclinical and clinical evidence of SHBG as an antimalarial target are present, these findings may indicate 2-(4a,8-Dimethyl-6-oxo-1,2,3,4,4a,5,6,8a-octahydro-naphthalen-2-yl)-propionaldehyde ability in modulating SHBG activity to prevent hemolysis and hypoxia in malarial complications. 3',8,8'-Trimethoxy-3-piperidyl-2,2'-binaphthalene-1,1',4,4'-tetrone was found to produce the most stable interactions against PTGS2 with -7.8 kcal/mol binding affinity with highest number of matching amino acid interactions (Table 3 and 4). Prostaglandin Endoperoxidase Synthase 2 (PTGS2) or cyclooxygenase-2 (COX-2) regulates several inflammation-related domains of malaria pathophysiology and increases in *P. falciparum* infection, clinically manifested as monocyte upregulation, surging IL-10 levels, malarial anemia, and miscarriage in pregnant malarial patients.³⁴

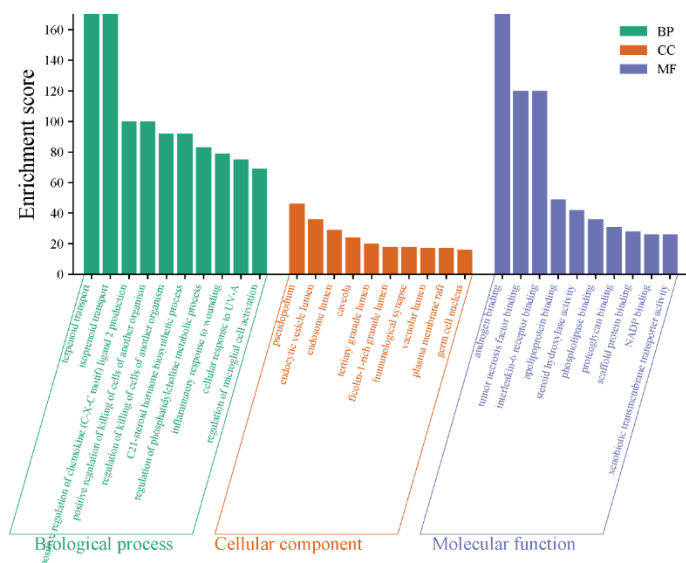


Figure 4: GO Analysis

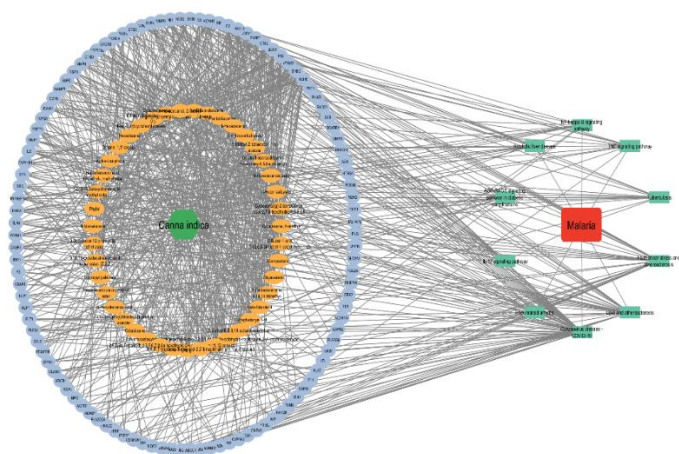


Figure 5: H-C-T-P-D Network

Previous study reported that artemisinin, first-line antimalarial agent, produced stable bond with PTGS2 with excellent binding affinity score (< -8.0 kcal/mol) and displayed interactions in several amino acid residues, including Tyr348, Val344, Leu534, Phe205, and Tyr385.³³ These findings indicate 3',8,8'-Trimethoxy-3-piperidyl-2,2'-binaphthalene-1,1',4,4'-tetrone may pose as a potential PTGS2 and anti-inflammatory agents in treating malaria.

3',8,8'-Trimethoxy-3-piperidyl-2,2'-binaphthalene-1,1',4,4'-tetrone exhibited the most table interaction (-7.7 kcal/mol) and showed two matching amino acid interactions towards Coagulation Factor X (F10) (Table 3 & 4). Coagulation Factor X (F10) is one of the vitamin K-dependent proteases that holds crucial role in coagulation cascade and key of thrombin generation. Malaria pathogenesis has been associated with alterations of blood coagulation that also determines the severity of malaria. Therefore, 3',8,8'-Trimethoxy-3-piperidyl-2,2'-binaphthalene-1,1',4,4'-tetrone demonstrated the potential to mitigate complications and to prevent the progression of malarial disease.³⁵

Finally, 3',8,8'-Trimethoxy-3-piperidyl-2,2'-binaphthalene-1,1',4,4'-tetrone was also found to have the lowest binding affinity (-10.6 kcal/mol) among other phytoconstituents and had two matching amino acids with the native ligand, Ala114 and Trp79, against Butyrylcholinesterase (BuChE) (Table 3 & 4). Butyrylcholinesterase (BuChE) is a non-specific cholinesterase mainly synthesized in the liver and often becomes as a target in malaria disease. Several drugs including chloroquine, hydroxychloroquine, and primaquine has been confirmed as antimalarial drugs for the anticholinesterase activity.³⁶ In another study, a first-line antimalarial drug, artemisinin, was found to

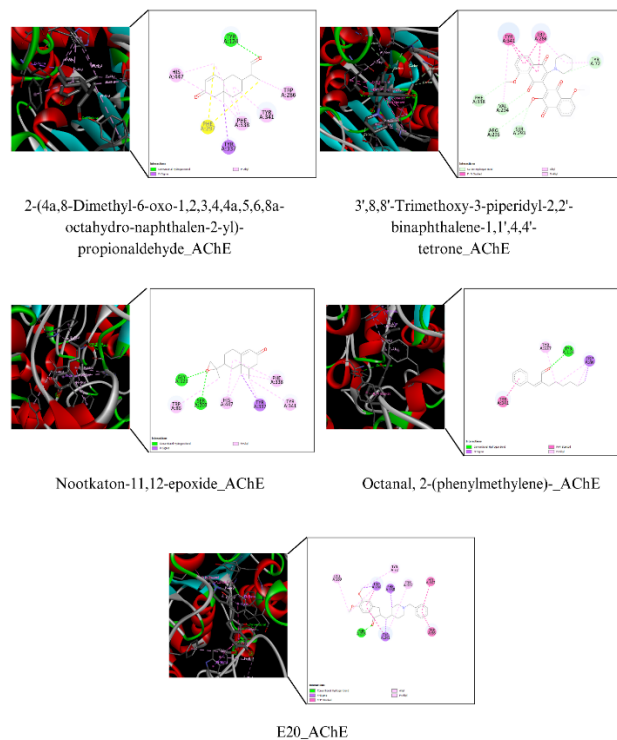


Figure 6: AChE Docking 2D and 3D Visualization

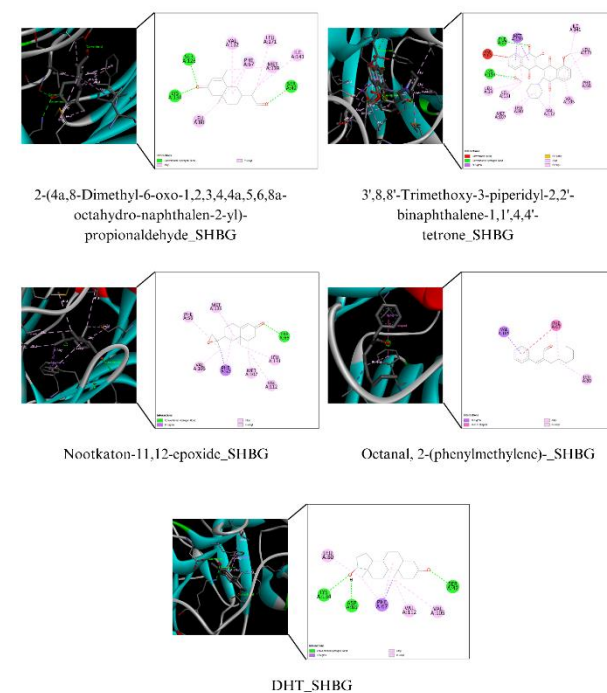


Figure 7: SHBG Docking 2D and 3D Visualization

perform hydrogen bond interactions with the residues of Gly116 and Gly117 along with hydrophobic interactions with His438, Trp82, and Phe329. In addition, artemisinin showcased low binding energy against the target protein, indicating the stable binding.³⁷ Hence, these findings reveal the potential of 3',8,8'-Trimethoxy-3-piperidyl-2,2'-binaphthalene-1,1',4,4'-tetrone as a potent modulator of BuChE and exhibits antimalarial activity.

Table 4. Amino Acid Interactions

Target	Compound	Amino Acid Interactions
ACHE	2-(4a,8-Dimethyl-6-oxo-1,2,3,4,4a,5,6,8a-octahydro-naphthalen-2-yl)-propionaldehyde	Conventional hydrogen bond: Tyr124 Pi-sigma: Tyr337 Pi-alkyl: His447, Trp286, Tyr341, Phe338, Phe297 Carbon-hydrogen bond: Tyr72, Ser293, Val294, Phe338 Pi-pi stacked: Tyr341, Trp286, Arg296 Alkyl: Val294 Pi-alkyl: Tyr341, Trp286, Tyr72, Phe338
	3',8,8'-Trimethoxy-3-piperidyl-2,2'-binaphthalene-1,1',4,4'-tetrone	Conventional hydrogen bond: Ser203, Gly121 Pi-sigma: Tyr337 Pi-alkyl: Phe338, Tyr341, Tyr337, His447, Trp86
	Nootkaton-11,12-epoxide	Conventional hydrogen bond: Tyr124 Pi-sigma: Trp86 Pi-pi stacked: Tyr341 Pi-alkyl: Trp86, Tyr337
	Octanal, 2-(phenylmethylene)-	Conventional hydrogen bond: Phe295 Pi-sigma: Trp286, Phe338, Tyr341 Pi-pi stacked: Trp286, His447, Trp86, Tyr341 Alkyl: Leu289 Pi-alkyl: Tyr72, Trp286, Tyr337, Tyr341
	E20 (native)	Conventional hydrogen bond: Ser128, Ser42, Lys134 Alkyl: Val112, Leu171, Met139, Ile141, Leu80 Pi-alkyl: Phe67 Unfavorable bump: Asp65 Conventional hydrogen bond: Lys134, Phe67 Pi-sigma: Met139 Pi-sulfur: Met139 Alkyl: Ile141, Leu171, Val112, Leu80, Met107, Leu131, Leu34, Lys134, Met139 Pi-alkyl: Leu171, Phe56, Val105, Val112
SHBG	2-(4a,8-Dimethyl-6-oxo-1,2,3,4,4a,5,6,8a-octahydro-naphthalen-2-yl)-propionaldehyde	Conventional hydrogen bond: Trp66 Pi-sigma: Phe67 Alkyl: Met139, Leu131, Val112, Met107, Val105 Pi-alkyl: Phe67, Phe56 Pi-sigma: Val105 Pi-pi T-shaped: Phe67 Alkyl: Leu80 Pi-alkyl: Phe67
	3',8,8'-Trimethoxy-3-piperidyl-2,2'-binaphthalene-1,1',4,4'-tetrone	Conventional hydrogen bond: Ser42, Asp65, Lys134 Pi-sigma: Phe67 Alkyl: Leu80, Val105, Val112 Pi-alkyl: Phe67
	Nootkaton-11,12-epoxide	Conventional hydrogen bond: Thr206 Pi-sigma: His386 Pi-alkyl: His386, His207, His214 Pi-sigma: Leu294 Pi-pi stacked: His386 Alkyl: Val291, Leu294, Val295 Pi-alkyl: Leu294, Val447, His207, His388, His386
	Octanal, 2-(phenylmethylene)-	Conventional hydrogen bond: Thr206 Pi-sigma: His388 Alkyl: Leu391, Val295 Pi-alkyl: His388, His207
	DHT (native)	Conventional hydrogen bond: Gln203 Carbon-hydrogen bond: His207 Pi-pi stacked: His386 Alkyl: Ala202, Leu390 Pi-alkyl: His388, Trp387, Tyr385
PTGS2	2-(4a,8-Dimethyl-6-oxo-1,2,3,4,4a,5,6,8a-octahydro-naphthalen-2-yl)-propionaldehyde	Conventional hydrogen bond: Thr212, Gln454, Pi-donor hydrogen bond: Gln203 Pi-sigma: His386 Pi-pi stacked: His386 Pi-pi T-shaped: His207, His388 Alkyl: Val447, Leu294, Val295, Ile408, Leu391, Ala199, Ala202, Pi-alkyl: Val447, Tyr404, Leu391, Phe395, Phe210, His207, His388, Tyr385, Trp387
	3',8,8'-Trimethoxy-3-piperidyl-2,2'-binaphthalene-1,1',4,4'-tetrone	Conventional hydrogen bond: Thr215 Pi-sigma: Trp215, Phe174
	Nootkaton-11,12-epoxide	
	Octanal, 2-(phenylmethylene)-	
	COH (native)	
F10	2-(4a,8-Dimethyl-6-oxo-1,2,3,4,4a,5,6,8a-octahydro-naphthalen-2-yl)-propionaldehyde	

	3',8,8'-Trimethoxy-3-piperidyl-2,2'-binaphthalene-1,1',4,4'-tetrone	Pi Sulfur: Cys220, Conventional hydrogen bond: Gly219 Alkyl: Ala195 Pi-alkyl: His57, Tyr99, Phe174 Pi-pi stacked: Tyr99, Phe174 Pi-sigma: Trp215 Pi-alkyl: Trp215, Tyr99, Phe174
	Nootkaton-11,12-epoxide	
	Octanal, 2-(phenylmethylene)-	Pi-alkyl: His57, Tyr99 Alkyl: Ala195 Pi-pi T shaped: Trp215 Pi-pi stacked: Tyr99 Carbon hydrogen bond: Lys96, Gln192 Alkyl: Val213, Ala190 Pi-alkyl: Tyr228, Ala190, Trp215, Tyr99, Phe174 Amida Pi-stacked: Cys191, Trp215 Conventional hydrogen bond: Gly216 Unfavorable donor-donor: Gly216 Pi-pi stacked: Trp215 Pi-pi T-shaped: Tyr99, Phe174 Conventional hydrogen bond: Gly5, Tyr18
Native		
BuCHE	2-(4a,8-Dimethyl-6-oxo-1,2,3,4,4a,5,6,8a-octahydro-naphthalen-2-yl)-propionaldehyde	
	3',8,8'-Trimethoxy-3-piperidyl-2,2'-binaphthalene-1,1',4,4'-tetrone	Pi-pi T shaped: Tyr118 Alkyl: Ala114, Met33 Pi-alkyl: Trp26, Trp79, Ala1 Carbon hydrogen bond: His34 Pi-pi T-shaped: His34, Trp17, Unk8 Pi-cation: His34 Conventional hydrogen bond: Tyr79, Tyr18 Pi-alkyl: Tyr79
	Nootkaton-11,12-epoxide	
	Octanal, 2-(phenylmethylene)-	Conventional hydrogen bond: Ala1 Pi-alkyl: Trp79, His34, Leu72 Pi-sigma: Trp79 Pi-pi T-shaped: Phe115, Trp17 Conventional hydrogen bond: His34 Pi-pi stacked: His34, Trp79 Pi-alkyl: Trp79 Alkyl: Ala114
	Native	

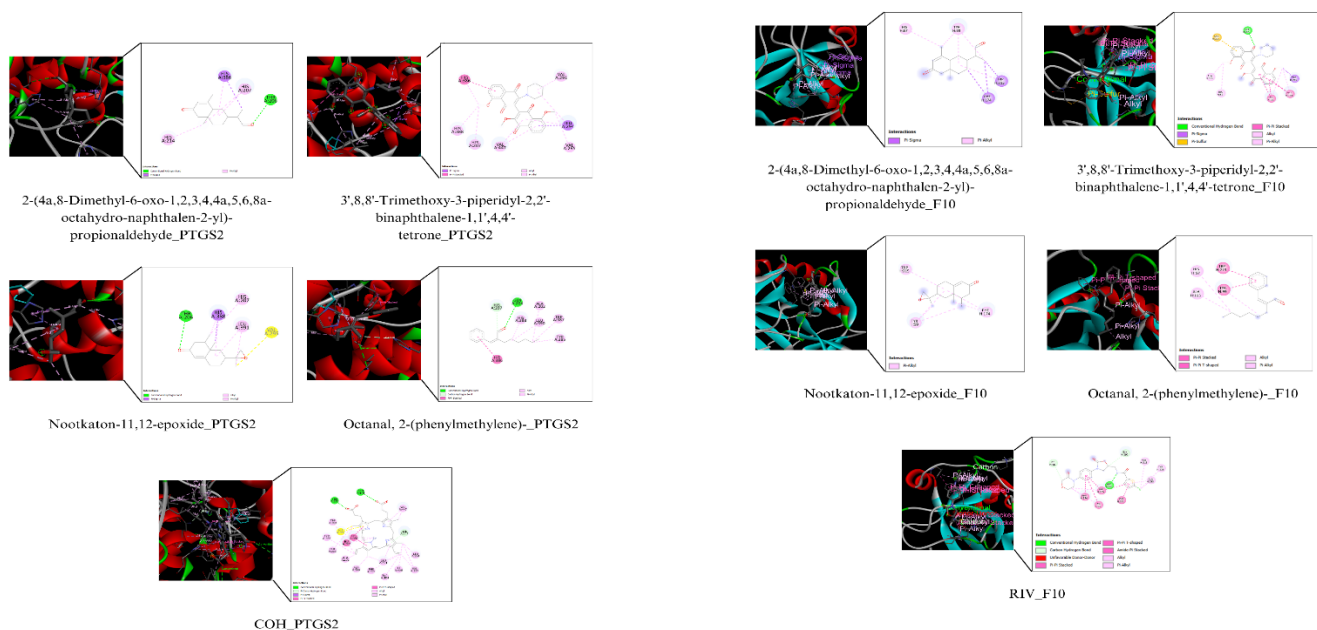


Figure 8: PTGS2 Docking 2D & 3D Visualization

Figure 9: F10 Docking 2D & 3D Visualization

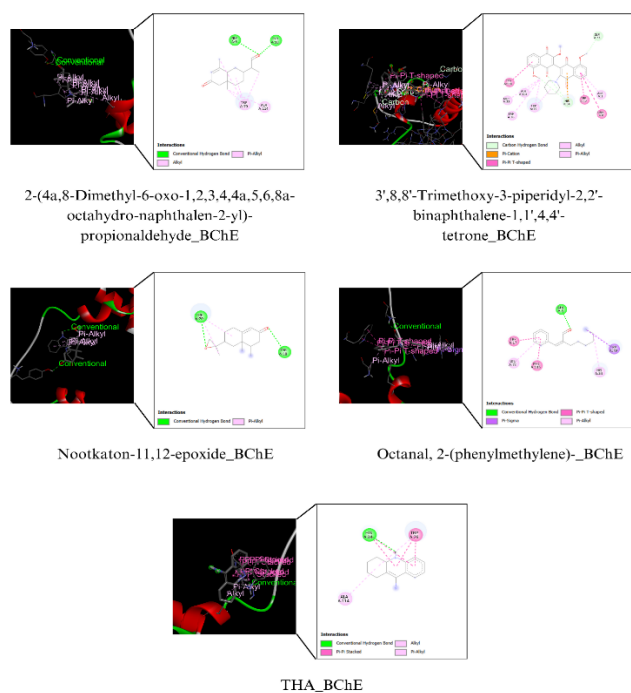


Figure 10: BChE Docking 2D & 3D Visualization

Conclusion

The findings from this study highlight the promising antimalarial potential of *Canna indica* through its active compounds, which demonstrated significant binding with target proteins relevant to malaria pathology. This supports the use of *C. indica* as a natural therapeutic candidate for malaria, warranting further research into its mechanisms and efficacy in clinical settings.

Conflict of Interest

The authors declare no conflict of interest.

Author's Declaration

The authors hereby declare that the work presented in this article are original and that any liability for claims relating to the content of this article will be borne by them.

Acknowledgement

We thank the Faculty of Medicine, Universitas Brawijaya Malang, for providing the research funding.

References

- Marrelli MT, Brotto M. The effect of malaria and anti-malarial drugs on skeletal and cardiac muscles. *Malar J*. 2016; 15:1–6. Doi: <https://doi.org/10.1186/s12936-016-1577-y>.
- González-Sanz M, Berzosa P, Norman FF. Updates on malaria epidemiology and prevention strategies. *Curr Infect Dis Rep*. 2023; 25:131–139. Doi: <https://doi.org/10.1007/s11908-023-00805-9>.
- Fikadu M, Ashenafi E. Malaria: An overview. *Infect Drug Resist*. 2023; 16:3339–3347. Doi: <https://doi.org/10.2147/IDR.S405668>.
- Varo R, Chaccour C, Bassat Q. Update on malaria. *Med Clin (Barc)*. 2020; 155:395–402. Doi: <https://doi.org/10.1016/j.medcli.2020.05.010>.
- Murugesan R, Kaleeswaran B. *In silico* drug discovery: Unveiling potential targets in *Plasmodium falciparum*. *Asp. Mol. Med.* 2024; 3:1-10. Doi: <https://doi.org/10.1016/j.amolm.2024.100038>.
- Doshi K, Pandya N, Datt M. *In silico* assessment of natural products and approved drugs as potential inhibitory scaffolds targeting aminoacyl-tRNA synthetases from *Plasmodium*. *Biotech*. 2020; 10:470-481. Doi: <https://doi.org/10.1007/s13205-020-02460-6>.
- Anh LT, Hieu N, Trang DT, Tai BH, Kiem PV. Two new acylated sucroses from the roots of *Canna indica* L. and their antioxidant activity. *Nat. Prod. Commun.* 2021; 16(2):1-5. Doi: <https://doi.org/10.1177/1934578X21991720>.
- Li L, Yang L, Yang LQ, He CR, He YX, Chen LP, Dong Q, Zhang HY, Chen SY, Li P. Network pharmacology: A bright guiding light on the way to explore the personalized precise medication of traditional Chinese medicine. *Chin. Med.* 2023; 18:146-164. Doi: <https://doi.org/10.1186/s13020-023-00853-2>.
- Fitrianiingsih AA, Santosaningsih D, Djajalaksana S, Muti'ah R, Lusida MI, Karyono SS, Prawiro, SR. Network pharmacology and in silico investigation on *Saussurea lappa* for viral respiratory diseases. *Trop J Nat Prod Res.* 2024; 8(1):5889–5896. Doi: <https://doi.org/10.26538/tjnpr/v8i1.26>.
- Muti'ah R, Fitriyani, Ningrum SES, Arriziq MA. Exploring the potential of tamarillo (*Cyphomandra betacea* Cav) compounds for the treatment of type 2 diabetes mellitus: A network pharmacology study. *Trop J Nat Prod Res.* 2024; 8(10):8704–8709. Doi: <https://doi.org/10.26538/tjnpr/v8i10.13>.
- Shamim S, Munawar R, Rashid Y, Qadar MZ, Bushra R, Begum I, Imran M, Quds T. Molecular Docking: An insight from drug discovery to drug repurposing approach. In: Podlipnik C (Eds.). *Unraveling molecular docking – From theory to practice*. London: IntechOpen; 2024. 1-33 p.
- Kristianingsih A, Soetrisno, Reviono R, Wasita B. Molecular docking study of quercetin from ethanol extract of *Mimosa pudica* Linn. on asthma biomarkers. *Trop J Nat Prod Res.* 2024; 8(10):8640–8645. Doi: <https://doi.org/10.26538/tjnpr/v8i10.4>.
- Nugraha RYB, Faratisha IFD, Mardhiyyah K, Ariel DG, Putri FF, Nafisatuzzamrudah, Winarsih S, Sardjono TW, Fitri, LE. Antimalarial properties of isoquinoline derivative from *Streptomyces hygroscopicus* subsp. *Hygroscopicus*: An *in silico* approach. *Biomed Res Int* 2020; 6135696:1-15. Doi: <https://doi.org/10.1155/2020/6135696>.
- Ijoma IK, Okafor CE, Ajiwe VIE. Computational studies of 5-methoxypsolaren as potential deoxyhemoglobin s polymerization inhibitor. *Trop J Nat Prod Res.* 2024; 8(10):8835–8841. Doi: <https://doi.org/10.26538/tjnpr/v8i10.28>.
- Daina A, Michielin O, Zoete V. SwissADME: A free web tool to evaluate pharmacokinetics, drug-likeness and medicinal chemistry friendliness of small molecules. *Sci Rep*. 2017; 7(1):1-13. Doi: <https://doi.org/10.1038/srep42717>.
- Benet LZ, Hosey CM, Ursu O, Oprea TI. BDDCS, the rule of 5 and drugability. *Adv Drug Deliv Rev.* 2016; 101:89–98. Doi: <https://doi.org/10.1016/j.addr.2016.05.007>.
- Adianingsih OR, Fajrin FF, Johan CK. Exploring the mechanism of Glycyrrhiza glabra and Curcuma domestica against skin photoaging based on network pharmacology. *Indones J Biotechnol.* 2024; 29:98–110. Doi: <https://doi.org/10.22146/ijbiotech.93332>.
- Tang D, Chen M, Huang X, Zhang G, Zeng L, Zhang G, Wu S, Wang Y. SRplot: A free online platform for data visualization and graphing. *PLoS One.* 2023; 18:1-8. Doi: <https://doi.org/10.1371/journal.pone.0294236>.
- Zhou Y, Zhou B, Pache L, Chang M, Khodabakhshi AH, Tanaseichuk O, Benner C, Chanda S. Metascape provides a biologist-oriented resource for the analysis of systems-level datasets. *Nat Commun.* 2019; 10(1):1-10. Doi: <https://doi.org/10.1038/s41467-019-09234-6>.

20. Cheng X, Song Z, Wang X, Xu S, Dong L, Bai J, Li G, Zhang C. A network pharmacology study on the molecular mechanism of protocatechualdehyde in the treatment of diabetic cataract. *Drug Des Devel Ther.* 2021; 15:4011–4023. Doi: <https://doi.org/10.2147/DDDT.S334693>.
21. Xiang C, Liao Y, Chen Z, Xiao B, Zhao Z, Li A, Xia Y, Wang P, Li H, Xiao T. Network pharmacology and molecular docking to elucidate the potential mechanism of Ligusticum Chuanxiong against osteoarthritis. *Front Pharmacol.* 2022; 13:1–13. Doi: <https://doi.org/10.3389/fphar.2022.854215>.
22. Hema K, Ahamad S, Joon HK, Pandey R, Gupta D. Atomic resolution homology models and molecular dynamics simulations of plasmodium falciparum tubulins. *ACS Omega.* 2021; 6:17510–17522. Doi: <https://doi.org/10.1021/acsomega.1c01988>.
23. Bell EW, Zhang Y. DockRMSD: An open-source tool for atom mapping and RMSD calculation of symmetric molecules through graph isomorphism. *J Cheminform* 2019; 11:40-48. Doi: <https://doi.org/10.1186/s13321-019-0362-7>.
24. Deshpande RR, Tiwari AP, Nyayanit N, Modak M. *In silico* molecular docking analysis for repurposing therapeutics against multiple proteins from SARS-CoV-2. *Eur J Pharmacol.* 2020; 886:1-15. Doi: <https://doi.org/10.1016/j.ejphar.2020.173430>.
25. Traore K, Arama C, Medebielle M, Doumbo O, Picot S. Do advanced glycation end-products play a role in malaria susceptibility? *Parasite* 2016; 23:15-24. Doi: <https://doi.org/10.1051/parasite/2016015>.
26. Baska P, Norbury LJ. The role of nuclear factor kappa B (NF-κB) in the immune response against parasites. *Pathogens.* 2022; 11:310-333. Doi: <https://doi.org/10.3390/pathogens11030310>.
27. Scherer EF, Cantarini DG, Siqueira R, Ribeiro EB, Braga ÉM, Honório-França AC, França EL. Cytokine modulation of human blood viscosity from vivax malaria patients. *Acta Trop* 2016; 158:139–147. Doi: <https://doi.org/10.1016/j.actatropica.2016.03.001>.
28. Otterdal K, Berg A, Michelsen AE, Patel S, Gregersen I, Sagen EL, Halvorsen B, Yndestad A, Ueland T, Langeland N, Aukrust P. Plasma levels of interleukin 27 in falciparum malaria is increased independently of co-infection with HIV: Potential immune-regulatory role during malaria. *BMC Infect Dis* 2020; 20:65-75. Doi: <https://doi.org/10.1186/s12879-020-4783-8>.
29. Sloop GD, De Mast Q, Pop G, Weidman JJ, St. Cyr JA. The role of blood viscosity in infectious diseases. *Cureus.* 2020; 12(2):1-11. Doi: <https://doi.org/10.7759/cureus.7090>.
30. Rants'o TA, van Greunen DG, van der Westhuizen CJ, Riley DL, Panayides JL, Koekemoer LL, Zyl RLV. The *in silico* and *in vitro* analysis of donepezil derivatives for *Anopheles* acetylcholinesterase inhibition. *PLoS One* 2022; 17(11):1-21. Doi: <https://doi.org/10.1371/journal.pone.0277363>.
31. Chougouo RDK, Nguekeu YMM, Dzoyem JP, Awouafack MD, Kouamouo J, Tane P, McGaw LJ, Eloff JN. Anti-inflammatory and acetylcholinesterase activity of extract, fractions and five compounds isolated from the leaves and twigs of *Artemisia annua* growing in Cameroon. *Springerplus.* 2016; 5(1):1525-1531. Doi: <https://doi.org/10.1186/s40064-016-3199-9>.
32. John L, Vijay R. Role of TAM receptors in antimalarial humoral immune response. *Pathogens.* 2024; 13(4):298-312. Doi: <https://doi.org/10.3390/pathogens13040298>.
33. Guo Y, Li Z, Cheng N, Jia X, Wang J, Ma H, Zhao R, Li B, Cai Y, Yang Q. To investigate the effects of artemisinin on inflammatory factors and intestinal microbiota in rats with ulcerative colitis based on network pharmacology. *Front. Gastroenterol.* 2022; 1:1-17. Doi: <https://doi.org/10.3389/fgstr.2022.979314>.
34. Wang X, Chen J, Zheng J. The roles of COX-2 in protozoan infection. *Front. Immunol.* 2023; 14:1-13. Doi: <https://doi.org/10.3389/fimmu.2023.955616>.
35. Riedl J, Mordmüller B, Koder S, Pabinger I, Kremsner PG, Hoffman SL, Ramharther M, Ay C. Alterations of blood coagulation in controlled human malaria infection. *Malar J.* 2016; 15:15-21. Doi: <https://doi.org/10.1186/s12936-015-1079-3>.
36. Bosak A, Opsenica DM, Šinko G, Zlatar M, Kovarik Z. Structural aspects of 4-aminoquinolines as reversible inhibitors of human acetylcholinesterase and butyrylcholinesterase. *Chem Biol Interact* 2019; 308:101–109. Doi: <https://doi.org/10.1016/j.cbi.2019.05.024>.
37. Barrientos RE, Romero-Parra J, Cifuentes F, Palacios J, Romero-Jola NJ, Paredes A, Varagas-Arana G, Simirgiotis MJ. Chemical fingerprinting, aorta endothelium relaxation effect, and enzymatic inhibition of canelo (*Drimys winteri* J. R. Forst. & G. Forst, (D.C) A. Gray, family Winteraceae) fruits. *Foods.* 2023; 12(13):2580-2598. Doi: <https://doi.org/10.3390/foods12132580>.